



Hydrogeological characteristics and water chemistry in a coastal aquifer of Korea: implications for land subsidence

Jiwook Jang · Jin-Yong Lee ·
Mostafa Redwan · Maimoona Raza ·
Minwook Lee · Serim Oh

Received: 15 July 2023 / Accepted: 30 September 2023 / Published online: 12 October 2023
© The Author(s), under exclusive licence to Springer Nature Switzerland AG 2023

Abstract Land subsidence is the gradual or sudden dropping of the ground surface developed by increasing the total stress. Most studies have discussed the relationship between land subsidence with groundwater level. However, there is a lack of discussion on groundwater environmental changes after occurring land subsidence. This study aimed to evaluate the hydrogeological and water chemistry characteristics of construction sites with land subsidence. Land subsidence in the Yangyang coastal area occurred suddenly on August 3, 2022, when the retaining wall of the construction collapsed. The groundwater level was measured three times, and water samples were collected

twice between August 5, 2022, and September 5, 2022, for laboratory analysis. After land subsidence occurred, the average groundwater level was -19.91 m ground level (GL) on August 9, 2022, and finally decreased to -19.21 m GL on September 05, 2022. The groundwater levels surrounding the construction site gradually increased for a month. The electrical conductivity value measured at the monitoring wells ranged from 89 to 7800 $\mu\text{S}/\text{cm}$, and four wells exceeded the measurement limit near the groundwater leaked points. The highest mixing ratio of leaked water samples, collected on August 9, 2022, was 27.6%. Furthermore, the fresh groundwater-saltwater interface depth was estimated to be above the construction bottom. Although groundwater levels recovered, the groundwater quality continuously is affected by saltwater. This finding could contribute to understanding the hydrogeological characteristics surrounding construction sites with land subsidence and provide insight into the hydrochemical evolution process during declined groundwater levels in coastal aquifers.

J. Jang · J.-Y. Lee (✉) · M. Raza · M. Lee · S. Oh
Department of Geology, College of Natural Sciences,
Kangwon National University, Chuncheon 24341,
Republic of Korea
e-mail: hydrolee@kangwon.ac.kr

J. Jang
e-mail: jjwook1108@kangwon.ac.kr

M. Raza
e-mail: maimoonaraza14@gmail.com

M. Lee
e-mail: minwooklee@kangwon.ac.kr

S. Oh
e-mail: serimoh@kangwon.ac.kr

M. Redwan
Geology Department, Sohag Faculty of Science, Sohag
University, Nasser City 82524, Egypt
e-mail: mostafa.redwan@science.sohag.edu.eg

Keywords Land subsidence · Coastal aquifer · Groundwater level · Hydrochemistry · Republic of Korea

Introduction

Land subsidence (LS) is the gradual or sudden sinking of the ground surface caused by increased total

stress (Galloway et al., 1999). LS caused by changes in the underground environment has been studied since the early twentieth century and can result from various factors, including increased surface load, groundwater pumping, drainage (Galloway et al., 1999; Herrera-García et al., 2021), and excavation of the ground surface (Galloway & Burbey, 2011; Galloway et al., 2016; Guzy & Malinowska, 2020; Marfai & King, 2007; Orhan, 2021; Xu et al., 2008, 2012). Excavation causes LS to lower the groundwater level and causes the salinization of water resources in coastal areas. Generally, seawater intrusion (or salt-water rise) can result in the salinization of domestic and agricultural water resources in coastal areas (Jiao & Post, 2019; Michael et al., 2017). Salinization of groundwater and soil is a global problem because it reduces the amount of available water resources and damages agricultural crops (Jeen et al., 2021).

Urbanization and tourism development increase groundwater pumping (Galloway et al., 1999), disrupting the balance between freshwater and saltwater, accelerating the aquifer salinization (Cardona et al., 2004), and exacerbating the problem. In addition, LS significantly affects people's lives, particularly in urban areas, where it can lead to the collapse of buildings and frequent flooding in low-lying regions (Shirzaei et al., 2021). Once LS occurs, it is not naturally recoverable and can be costly to restore (Galloway et al., 1999; Phien-vej et al., 2006). In recent years, the underground environment in urban areas has been greatly impacted by building construction. Consequently, many countries have faced LS hazards from urbanization since the twentieth century. LS in urban areas can significantly damage human lives and assets.

In East Asia, LS is commonly reported in unconsolidated sediments comprising fine grains, which are typically located near streams, lakes, and oceans (Bagheri-Gavkosh et al., 2021; Yan et al., 2022). Some of the countries facing such problems include China, Japan, and Thailand. LS occurred especially in coastal cities, the low-lying land of the plains, and basins such as Bangkok and Tianjin. In particular, Shanghai (located on the southern estuary of the Yangtze River in eastern China and China's financial and commercial hub) was offered soft deposits from the Yangtze River, with a surface elevation of 2.2–4.5 m (Wei et al., 2010). These deposits are loose with a thickness of 200–320 m (Xu et al.,

2017). In these cases, the LS gradually occurred at a depth of 75 m during the 1990s through the extraction of groundwater from thick and soft deposits (Gong et al., 2009). In Shanghai, dewatering systems comprise retaining walls which are buried cutoffs shaped in the middle of confined aquifers. Shanghai LS was caused by groundwater extraction for the stabilization of the soil and retaining walls. According to Wu et al. (2018), Tianjin (a major city in North China that is 137 km southeast of Beijing, located along the Hai River, which connects to the Yellow and Yangtze Rivers) has a soft soil deposit (silt, sand, silty clay, and clay) of quaternary sediments approximately 100–430 m thick. The LS in Tianjin was caused by excessive groundwater pumping for urban construction. Wu et al. (2018) reported that LS and various geohazards, such as water in-rushing, quicksand, and piping hazards, occur. To prevent LS, a dewatering block system, appropriate foundation pit construction, and dewatering are required. Excessive groundwater extraction is the main cause of most LS, and it frequently occurs in thick unconsolidated sediments. However, most previous studies have considered the groundwater level before the occurrence of the LS (CITYN, 2020), and the surrounding groundwater environment after the occurrence of the LS is lacking.

LS in coastal areas can increase the risk of seawater intrusion into aquifers, which can exacerbate water quality. The outcome is a significant reduction in freshwater availability, leading to damage to agricultural activities and organisms. Therefore, it is imperative to consider seawater intrusion and LS in coastal management and planning to protect freshwater resources and effectively mitigate potential hazards. Seawater intrusion and LS are complex issues requiring a comprehensive and integrated approach to address them. This includes geophysical and geological factors and the social, economic, and environmental aspects of the problem to develop effective management strategies.

In recent years, there has been an increasing trend in high-rise buildings in coastal areas due to increased ocean tourism. However, research on hydrogeological assessments of excavations in coastal areas remains insufficient. This study aimed to evaluate the impact of excavation pits and LS in a coastal area on the hydrogeology of the surrounding area. The hydrogeology and engineering systems for waterproofing the construction area are described, and the effects of the

LS around the excavation pit on the groundwater system are evaluated using hydrogeological and hydrochemical approaches.

Study area

Location and geological characteristics

The study area is Yangyang, located in the coastal region of the Gangwon Province in the Republic of Korea, 150 km east of the capital city Seoul (Fig. 1). The extent of Yangyang County is 629.1 km², and the extent of the constructed site is 2.1 km². In this study, only four of the flowed-out groundwater and fourteen of the groundwater level wells around the constructed site were considered. The geological setting of Yangyang comprises Precambrian metamorphic rocks intruded by Jurassic igneous rocks (Park et al., 1997; Song et al., 2011; Fig. 1a). Quaternary alluvial deposits are unconformably overlying the metamorphic rocks. The metamorphic rocks of the Precambrian

era are complex and comprise biotite gneiss, leucogneiss, and granitic gneiss, which originated from volcanic bodies and porphyroblastic gneiss. Metamorphic rocks generally contain a low biotite content; however, the content varies significantly in the study area. They exhibit a partially banded structure with a well-developed gneiss structure. Jurassic igneous intrusion rocks are referred to as Yangyang igneous rocks and comprise medium-textured hornblende-biotite-granite that intrudes into biotite gneiss. Furthermore, Yangyang granite has significant amounts of alkaline-to-neutral xenoliths and an equigranular texture. Additionally, most of the study area comprises Quaternary alluvial deposits with an estimated thickness of 17–24 m. The artificial fill has a thickness of 2 m in the upper part of the Quaternary alluvial deposits. The Quaternary alluvial fan deposits mostly comprise a moraine layer with a thin clay layer at a depth of 14–17 m. The Quaternary alluvial deposits are located on the top layer and are distributed in the coastal area and estuary of the Yangyang Namdaecheon, a river that flows into the coast.

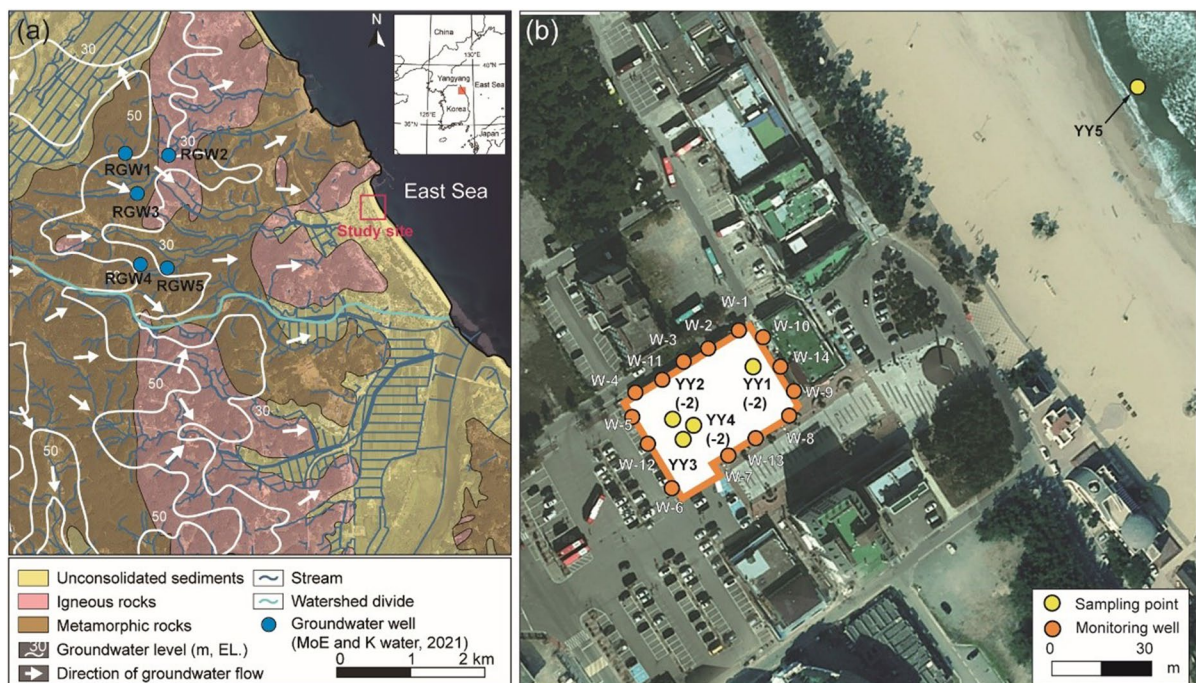


Fig. 1 Location of the study area showing geological map. **a** Geological setting with groundwater levels (blue circles mean the reference samples of groundwater) and **b** sampling points and monitoring wells

Hydrogeological characteristics

The study area is affected by a monsoon climate and receives rainfall originating from the East Sea. It typically experiences high temperatures and heavy rainfall between July and October. However, some regions have relatively low temperatures because they are located in mountainous areas. The annual mean air temperature in Yangyang from 2012 to 2021 was 11.1 °C, with a mean temperature of −3.5 °C in winter and 24.5 °C in summer. The annual mean precipitation is 1361.8 mm, with approximately 32.4 mm in winter and 317.7 mm in summer (<http://www.weather.rda.go.kr/>). The high summer precipitation is attributed to the influence of the Taebaek Mountains located west of Yangyang (Jang et al., 2022).

The study area is characterized by groundwater flowing from west to east, originating from the right side of the Taebaek Mountains located to the west (Fig. 1a). Groundwater near the coast is discharged into the East Sea as base flow. However, the precise groundwater flow velocity is unknown. The groundwater level is 2.7 m below the surface at an elevation of approximately 0.94 m (elevation level (EL)). The groundwater level in the Yangyang area is similar to the surface level.

Before excavation, six boreholes were drilled at the construction site, and a hydraulic conductivity test was performed in the unconfined aquifer layer to estimate the hydraulic conductivity. The average hydraulic conductivity was 9.02×10^{-4} cm/s, with the lowest and highest values occurring in the clay (9.87×10^{-6} cm/s) and silty sand layers (3.85×10^{-3} cm/s), respectively. Groundwater flow direction and velocity were measured at two points located in the northeast and southwest. The main groundwater flow directions from the inland mountainous region were measured to be towards the coastline, with a mean degree of direction of 76.5°. The mean groundwater flow velocity was also measured to be 1.6×10^{-1} m/day.

The Yangyang area is adjacent to the East Sea, and tides can significantly affect its quality and groundwater level. As of 2021, the tide range in this area was −0.09–1.03 m. Due to the difference in tide range, the distance from the coast changes to an average of approximately 15 m inland from the study

area. The coastline is located approximately 150 m from the location where the LS occurred.

Building construction and LS event

Building construction started on June 8, 2021, and will be completed on February 1, 2024. The building will have 26 floors with a height of 72.95 m. Below the surface, a parking lot with approximately six floors will be built. The excavation process consisted of 14 gradual excavation stages to prevent collapse. In the first stage, a wall panel was installed and gradually excavated. The final excavation depth was set at −26.20 m EL, 2 m deeper than originally planned (Fig. 2). The cast in place (CIP) with H piles and the soil cement wall (SCW) were used for the retaining wall method and waterproof method, respectively. A wall panel was installed using the SCW method to increase the stability of the wall, and the inner wall of the excavation was reinforced with CIP and H beams. The CIP had a diameter of 600 mm, the SCW had a diameter of 800 mm, and the H piles were $350 \times 350 \times 12 \times 19$ mm.

The previous survey was conducted before building construction (Fig. 3). But there is no data for the underground environment. The initial groundwater level was measured using ten monitoring wells on November 20, 2021, and four new wells were installed on March 08, 2022. The LS occurred with a size of $8 \times 12 \times 5$ m (width, length, and depth) northeast of the construction site on August 3, 2022. The quicksand with groundwater between the fissures of the CIP collapsed at a depth of −8 to −10 m GL. The LS destroyed the nearest building and a water supply pipe; the Yangyang County controlled traffic in the neighborhood. After the LS, groundwater leaked into the construction site, but the exact amount of discharge could not be measured. Following a safety inspection after the LS, the authorities confirmed damage to the retaining wall and the infiltration of soil and groundwater into the construction site. However, water barriers were installed to prevent leaks into the construction site. In the case of the damaged water pipe after the 2nd field campaign, it is expected that it blocked the water pipe 2 h after the LS occurred and affected the initial

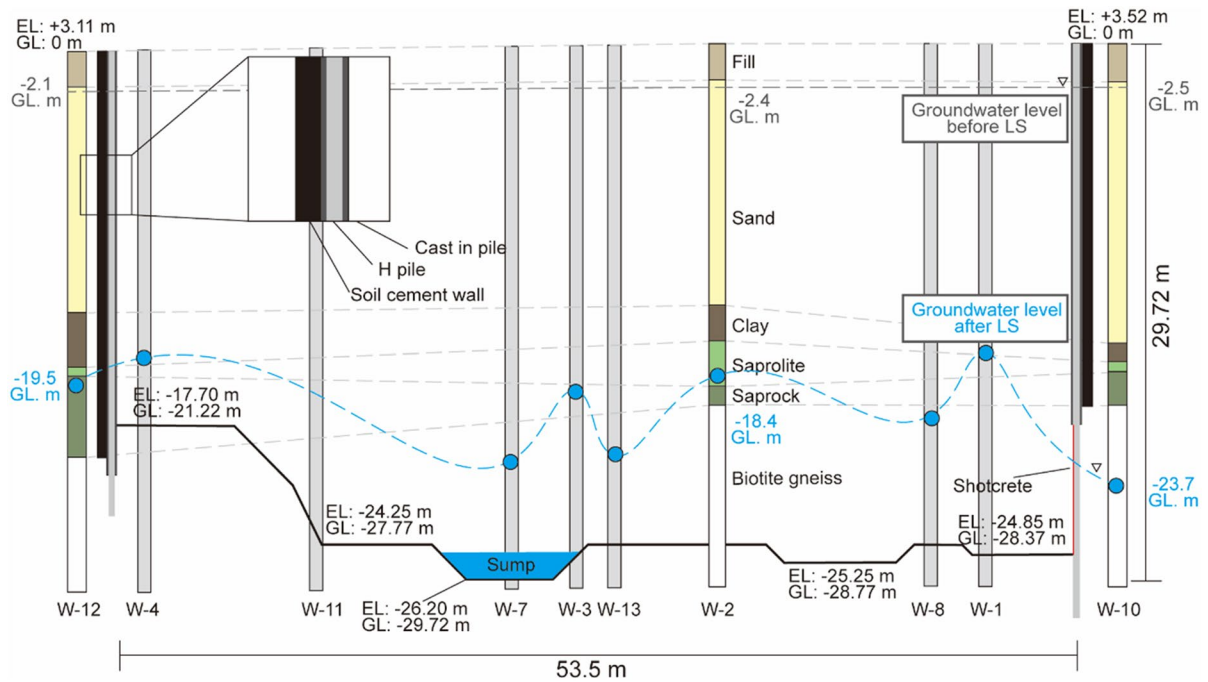
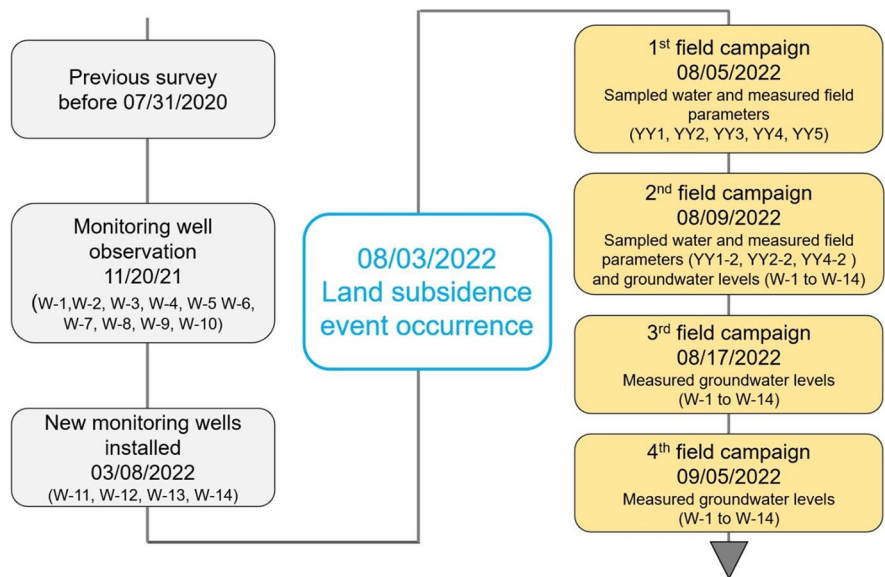


Fig. 2 Schematic showing waterproof systems with groundwater levels (cast-in-place pile, soil cement wall, shotcrete) and geological profile

Fig. 3 Flow chart of field campaign about the LS on the construction site in Yangyang



groundwater chemistry. After the installation of the water barrier on August 09, 2022, the LS was filled with sandy sediment and restored. Since it was impossible to collect groundwater samples,

only the groundwater level could be measured. However, LS occurred after the excavation was completed, leading to a decrease in the groundwater level in the surrounding area.

Methods and materials

Data collection

The geology of the study area was based on data from the Korea Institute of Geoscience and Mineral Resources in 2009. Hydrogeological data for the Yangyang area were obtained from the Basic Survey Report of Groundwater in Yangyang by the Ministry of Environment (MoE) and K-Water in 2021. The hydrogeological data were used to estimate the hydraulic conductivity and permeability of the aquifer. The hydraulic conductivity and geological cross section of the study site are described in the pre-construction survey report (CITYN, 2020). The groundwater level was described at intervals of 20 m, starting from 70 m; however, no groundwater monitoring wells were present at depths of ≤ 30 m; therefore, these points were not described (Fig. 1a). The groundwater level was measured twice monthly before the LS occurred; however, the records were found to be unreliable and were not considered in this study. Although some measurement records are available, some wells were either lost or poorly managed.

Field campaigns

Field campaigns were conducted four times following the occurrence of the LS on August 3, 2022 (Fig. 3). During the field campaigns, groundwater levels and field parameters were measured. Fourteen observation wells were installed around the construction site, including ten observation wells (W-1 to W-10) on November 20, 2021, and four new observation wells (W-11 to W-14) on March 8, 2022 (Fig. 1b). The observation well is 5 cm in diameter with a 30 m length, and the screen depth consists of a length of 1 m from the bottom. The groundwater levels were measured three times at each well using a Solinst 107 TLC meter with a detection limit of 80,000 $\mu\text{S}/\text{cm}$ and 5% accuracy, water temperature, and electrical conductivity (EC). EC and water temperature were measured and recorded at 1-m intervals from the surface to the bottom. Field parameters, including water temperature, pH, EC, oxidation–reduction potential (ORP), dissolved oxygen (DO), and turbidity, were measured, and samples were collected twice.

Water samplings and analysis

Samples were collected from three points (YY1, YY2, and YY3) where groundwater outflowed from the retaining wall and one point (YY4) where groundwater was discharged from the bottom of the sump. In addition, a sample was collected from the ocean located approximately 150 m from the construction site (YY5) to serve as a reference end member. In 2nd water sampling, samples were collected from three points within the construction site (YY1-2, YY2-2, and YY4-2) to compare the quality of the leaking groundwater.

After collection, the water samples were filtered through a 0.45- μm pore-sized membrane filter. The cation samples were adjusted to $\text{pH} < 2$ using hydrochloric acid and stored in polypropylene bottles, whereas the anion samples were stored in glass bottles. To prevent cross-contamination, all sample bottles were washed with distilled water prior to field campaigns in the laboratory. The samples were maintained at $< 4^\circ\text{C}$ and transported to the laboratory for analysis at the Korean Basic Science Institute in Ochang, Korea. The cations were analyzed using inductively coupled plasma-optical emission spectroscopy (Optima 8300, PerkinElmer, MA, USA), and the anions were analyzed using ion chromatography (Aquion, Thermo Fisher Scientific, MA, USA). YY5 (seawater) has a high EC and can potentially damage the equipment during analysis; therefore, it was diluted before analysis.

The water chemistry indices were used for the groundwater evolution process during the LS recovery activities. Also, these can be indicated that the underground environment changes in the study area. In this study, we used water chemical facies, ionic ratios (Na/Cl , Cl/Br), and BEX for dividing water chemistry indices. The water chemical facies are usually used for the determination of water dissolved ion composition (Piper, 1944). Additionally, base exchange indices (BEX) are used to indicate the water evolution process based on ionic relationships. They provide information on the extent of salinization (negative BEX values) or freshening (positive BEX values) reactions in the absence of dolomite aquifers. Furthermore, the shift of the freshwater-saltwater interface can be estimated using memory effects (Stuyfzand, 2008).

$$\text{BEX} = \text{Na}^+ + \text{K}^+ + \text{Mg}^{2+} - 1.0716\text{Cl}^- (\text{inmeq/L})$$

Results and discussion

Groundwater levels

The initial groundwater level was measured on November 20, 2021, and ranged from -3.46 to -3.29 m GL for wells W-1 to W-10 (Fig. 4). The lowest groundwater level was at W-10 (northeast of the construction site), and the highest groundwater level was at W-5 (west of the construction site). Normal groundwater flow was observed prior to the excavation. On March 8, 2022, when one new observation well was installed in each quadrant around the excavation site, the measured groundwater level ranged from -6.07 to -5.89 m GL, with W-14 closest to the sea having the lowest level and W-12 farthest from the sea having the highest. However, after the LS occurred, and the excavation level reached its maximum depth, the groundwater levels measured on August 9, 2022, were -24.35 m (lowest) at W-9 and -16.10 m (highest) at W-14 with an average of -19.91 m GL.

When the 3rd field campaign was on August 17, 2022, it could not be measured at W-11. The groundwater level decreased at seven other points and increased at six (W-7, W-8, W-9, W-13, and W-14) (Fig. 4). Among the points where the groundwater level increased, W-9 had the largest groundwater level change, with the groundwater level rising

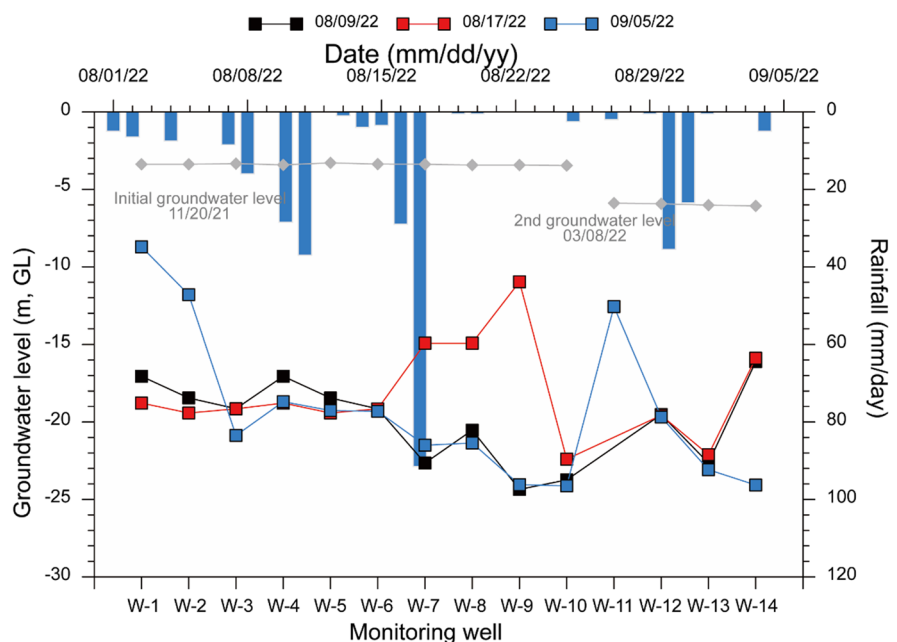
by approximately 10.97 m (the highest groundwater level was on August 17, 2022). The lowest measured groundwater level was -23.98 m GL at W-10, and the average groundwater level on the study site was -14.79 m GL. Subsequently, the groundwater level increased at three points (W-1, W-2, and W-11) and decreased at the other points. The three points where the groundwater level increased were located near the LS site, and it was estimated that the groundwater level recovered after the LS site was restored.

The average groundwater level measured on September 5, 2022, was -19.91 m GL. However, the average groundwater level in the 3rd field campaign (August 17, 2022) was presumed to have increased rapidly owing to rainfall. The average groundwater level of the 4th field campaign (September 5, 2022) is slowly recovering to -19.22 m GL.

The groundwater level at the construction site decreased (measured on March 08, 2022) as a result of the excavation, with an average decrease of approximately 3 m compared with the initial measurement taken prior to construction. The average groundwater level measured immediately after the LS was -19.91 m GL; however, it has been slowly increasing to -19.22 m GL.

At certain wells, the groundwater level increased rapidly after rainfall but fell again at the 3rd measurement when there was no rainfall. The groundwater

Fig. 4 Groundwater level change with increasing of the excavation depth at monitoring wells and daily rainfall during the study period



level in the area slowly recovered, particularly at the site where the accident occurred, as the LS was restored. These results correlated with the characteristics of the aquifers. The study area is an unconsolidated sediment layer with higher hydraulic conductivity (3.85×10^{-3} cm/s) than general bedrock aquifers, which can cause the groundwater level to increase and decrease faster than that for bedrock aquifers (Shen et al., 2020). In addition, the hydraulic conductivities of the partially included clay layer and saprock layer which were estimated at 9.87×10^{-6} cm/s and 7.10×10^{-5} cm/s, respectively. On the west side of the study area, a clay layer is deposited with a thickness of 3 m, and a saprock layer is deposited with a thickness of 4.5 m. On the other hand, at the point where the LS occurred, the clay layer was deposited relatively thinly, with a thickness of 1 m, and the saprock layer had a thickness of 2 m. It is presumed that groundwater level changes rapidly at the site where the LS occurred because it is deposited thinly unlike other sites. As shown in Fig. 2, the LS area comprises a thicker sand aquifer and a thinner clay aquifer than the other points. This indicates that a thin low-permeability layer and a thick layer with high hydraulic conductivity can affect the groundwater level. In Fig. 4, the results showed that the groundwater levels of W-3, W-4, W-5, and W-6, where the low hydraulic conductivity layer in the west of the study area was relatively thick, did not change rapidly during the study period.

Xu et al. (2014) suggested five groundwater descent patterns using FEM modeling based on the excavation depth and retaining wall. In particular, the drainage system in the excavation process penetrating the confined aquifer and aquitard could cause the groundwater level to drop; however, the change in the groundwater level of the unconfined aquifer was not expected to change significantly. However, these considerations were considered when a solid retaining wall completely excluded groundwater from the surrounding unconfined aquifer. In addition, in this excavation, the groundwater drainage system was not considered; however, natural seepage discharge was considered, and the reliability of the measurement of the surrounding unconfined surface aquifer was high.

In Shanghai, artificial cultivation was conducted to reduce the pumping water of the groundwater level to an extreme level and suppress the LS through artificial recharge after the LS (Shi et al., 2016). The

artificial cultivation began in 1966 to suppress LS, and an artificial cultivation of approximately 30×10^4 m³ was conducted in 1985. However, a groundwater level increase due to artificial recharge was observed, which could only be confirmed in the free-surface aquifer above the impervious layer. This suggests that the characteristics of the aquifer were not recovered because of the groundwater flow theory and the consolidation principle (Terzaghi, 1925) of the aquifer due to the LS. However, in this study, although the maintenance of the drainage system and inflow of nearby waterworks existed, the groundwater level only temporarily increased; however, over time, it decreased to the groundwater level immediately after LS. Although this was a temporarily large amount of recharge from the water supply pipe, it was judged to be due to the delay in moving to a nearby area.

Water chemistry

The EC of groundwater measured around the construction site during the 2nd field campaign was similar to general freshwater, except for three wells (W-4, W-5, and W-12) (Fig. 5). The EC was measured at 89–850 μ S/cm, indicating that it has the characteristics of freshwater (less than 2000 μ S/cm). However, the W-4, W-5, and W-12 wells displayed maximum values of 2910, 3253, and 7800 μ S/cm, respectively, indicating characteristics of saline or mixed with saline water, while W-4 and W-5 are located on the opposite side of the LS but have characteristics of saline water which are about 4.4 times higher than those measured around points W-4 and W-5. They are thought to have the characteristics of general fresh groundwater as it is the most distant point from the sea, but the measurements were unexpectedly high. In the case of W-12, the EC appears as low as 182 μ S/cm up to –21 m GL, but rises to about 7800 μ S/cm in the screen section. It is considered to be low on the upper part of the well because some surface rainfall flows into the upper part of the groundwater well, and high EC on the bottom surface where groundwater directly flows in. In addition, W-14 showed that the EC of the water surface was 800 μ S/cm, but as the water depth deepened, it gradually decreased to 300 μ S/cm and then rose to 500 μ S/cm at the bottom of the well. This is presumed to be due to the direct influx of surface materials (such as soil and contaminants through runoff), resulting in high electrical

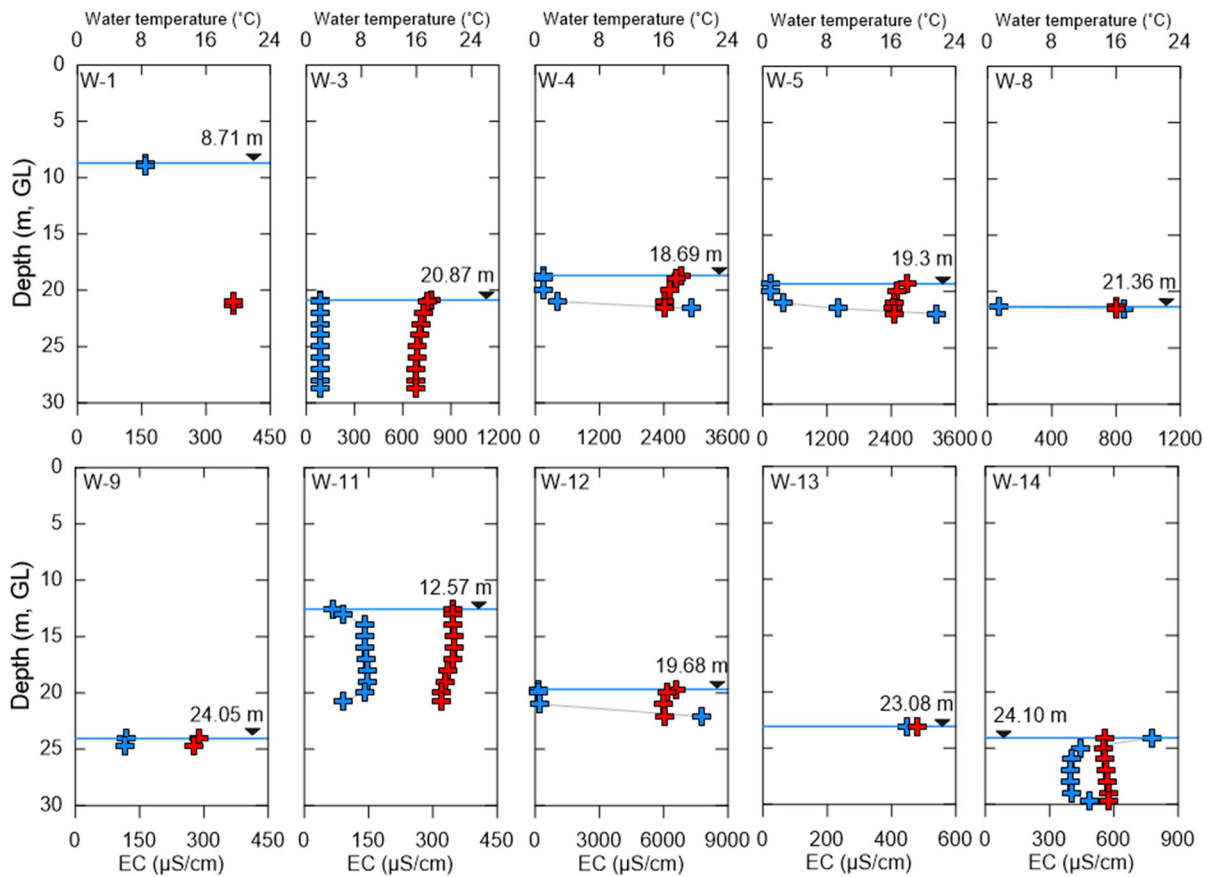


Fig. 5 Vertical distribution of electrical conductivity with groundwater depth (blue crosses mean electrical conductivity and red crosses mean water temperature)

conductivity characteristics on the surface of groundwater, and then gradually lowering general groundwater characteristics. Groundwater temperatures ranged from 15.4 to 23.1 °C. Most of them appeared similar to the water temperature of general groundwater, but in the case of the point where the groundwater level was high (W-3), the water temperature was higher due to contact with the atmosphere. The groundwater temperature in the study area was measured from the bottom, not in contact with the atmosphere, and the average water temperature was about 17.1 °C.

The EC can predict total dissolved solids in the groundwater, and it can be predicted in the case of samples that cannot be analyzed (small amounts of samples or cannot be collected). In particular, the EC measured at W-2, W-6, W-7, and W-10 exceeded the measurement limit (80,000 μS/cm). In particular, W-2 was affected by seawater despite being about 60 m

away from the LS, and W-6 and W-7, located around it, also appeared to be characterized by saline water mixing. This is presumed to be related to the outflow points of YY3 and YY4. In the case of 2 points, groundwater is leaking from the retaining wall, but from -7 to -8 m GL. It is also the point of continuous outflow in the cross section. It is presumed that saline water rises as the groundwater flows out, and thus, saline water flows into the observation well.

The pH of the groundwater at the construction site was slightly alkaline, ranging from 7.9 to 8.7. However, YY2-2 and YY4-2 had lower pH values of 7.5 and 7.8, respectively, while YY1-2 had a higher pH of 8.9 compared to YY1 (7.9). Additionally, the EC of YY1 decreased from 8159 to 2096 μS/cm. The increased pH in YY1 was likely a result of cement reinforcement or mixing with leaked tap water from a damaged water supply pipe. On the other hand, the

EC of other groundwater samples increased (YY2-2 and YY4-2), and YY2 (9443 $\mu\text{S}/\text{cm}$), indicating a highly mixed with saltwater. Furthermore, the DO of YY2-2 was influenced by deeper groundwater. Despite the increased EC of YY4-2, the DO increased due to continuous exposure to the atmosphere in the sump. The turbidity of YY4 significantly decreased from 62.2 to 22.1, indicating that the soil had flowed during the LS event stabilized and deposited over the study period. YY5 is a sample from the East Sea and showed minimal change throughout the study period.

In Shanghai, excessive pumping of groundwater over the long term has resulted in gradual LS. To prevent this, artificial recharging of tap water with groundwater in the area has begun (Shi et al., 2016). This study also changed the groundwater level by recharging with tap water at the construction site on the northeast side. It showed a temporary increase in the groundwater level, which decreased when the water supply pipe near the corresponding point was closed. In addition, as the TDS of the groundwater quality of the effluent near the corresponding point decreased, it was confirmed that the tap water was recharged.

Water samples were collected from three points (YY1, YY2, and YY3) where groundwater outflowed from the waterproof wall and one point where groundwater was discharged from the bottom of the sump (Table 1). In addition, dissolved ions and field parameter data investigated by the MoE and K-Water (2021) were used to investigate the quality of freshwater and groundwater in the study area and were compared with the groundwater

quality. The reference samples in the Yangyang area are of the Ca-HCO_3 type and are not contaminated (Fig. 6). This may be due to cation exchange processes where the Ca^{2+} from the freshwater Ca-HCO_3 replaces the Na^+ from the intruding saline water. The abundance of NaCl in the YY1–YY5 samples could signal high in the groundwater due to seawater intrusion. Some agricultural activities are conducted in the Yangyang coastal area. However, NO_3^- was not detected (ND) in three samples (RGW1, RGW2, and RGW5), while RGW3 and RGW4 had concentrations of 2.2 and 4.0 mg/L (Table 2). Cl^- is a common pollutant in domestic sewage (Raza & Lee., 2019) and is often associated with pollution. While it is a mountainous area, the anthropogenic impact was determined to be low (average Cl^- concentration: 9.22 mg/L) (An et al., 2023). Nevertheless, RGW1 and RGW4 have a higher Cl^- concentration than the other reference samples (Table 2). It is estimated that domestic sewage from nearby residents has flowed in. In the case of YY5, seawater samples separated by 150 m were used as end members. In the case of groundwater infiltration, the water temperature was lower compared to approximate groundwater, and the water temperature and pH were mostly adjusted at the point farthest from the seawater. Regarding EC, YY1, which was monitored at a point close to seawater, had the highest of 8159 $\mu\text{S}/\text{cm}$. Meanwhile, the groundwater quality inside the construction site is of the NaCl type as it approaches the shoreline. The construction site is approximately 150 m from the shoreline, and seawater intrusion is generated

Table 1 Physio-chemical field parameters of water samples measured in the study area

Sample	Date (mm/dd/yy)	Water temperature ($^{\circ}\text{C}$)	pH (SU)	*EC ($\mu\text{S}/\text{cm}$)	**DO (mg/L)	***ORP (mV)	Turbidity (NTU)
YY1	08/05/2022	17.8	7.9	8159	9.3	62	0.8
YY2	08/05/2022	17.4	8.2	1472	9.5	78	1.1
YY3	08/05/2022	19.3	8.7	4598	9.1	90	0.7
YY4	08/05/2022	19.2	8.1	13,731	8.5	119	62.2
YY5	08/05/2022	27.7	8.3	48,750	6.8	183	0.1
YY1-2	08/09/2022	19.6	8.9	2096	9.4	117	2.6
YY2-2	08/09/2022	19.6	7.5	9443	5.7	186	0.1
YY4-2	08/09/2022	20.4	7.8	15,487	9.7	163	22.1
YY5-2	08/09/2022	23.9	8.2	48,037	7.2	157	2.3

*EC electrical conductivity, **DO dissolved oxygen, ***ORP oxidation and reduction potential

Fig. 6 Chemical compositions of groundwater in the construction site and the reference samples in Yangyang (RGW mean the reference samples. And the reference samples from Moe and K-water, 2021)

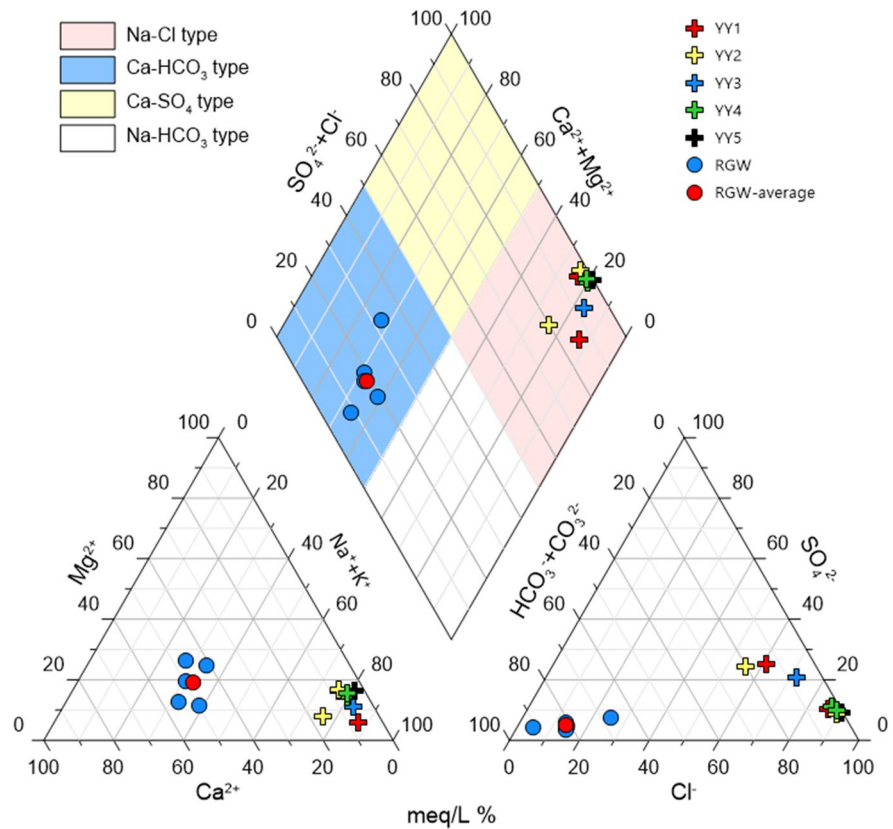


Table 2 Chemical compositions of water samples in the excavation site and reference samples of Yangyang (reference samples from MoE and K-water, 2021; units of all parameters are mg/L)

Sample	Na ⁺	Mg ²⁺	Ca ²⁺	K ⁺	Cl ⁻	HCO ₃ ⁻	SO ₄ ²⁻	NO ₃ ⁻
YY1	1141.0	136.3	102.7	75.2	1931.7	148.9	325.4	2.5
YY2	189.8	11.4	37.3	16.1	226.9	141.4	138.5	7.1
YY3	764.3	56.4	50.7	47.8	1017.8	171.9	407.7	12.0
YY4	2043.0	203.1	138.5	123.7	3817.9	162.3	691.0	3.5
YY5	9356.0	1039.8	322.6	501.2	17,763.1	129.9	2488.5	14.2
YY1-2	380.2	14.2	28.5	15.8	413.3	150.2	236.6	7.2
YY2-2	1617.2	196.6	135.6	68.1	3046.3	128.1	413.6	6.9
YY4-2	2844.0	302.8	177.7	107.0	4908.3	157.5	764.5	5.6
RGW1	14.9	3.2	22.6	8.6	10.8	107.5	5.0	*ND
RGW2	10.4	5.8	16.7	1.3	16.5	76.6	7.0	*ND
RGW3	9.2	3.5	14.3	1.6	6.1	66.0	4.0	2.2
RGW4	11.3	2.6	18.4	1.4	8.8	88.6	3.0	4.0
RGW5	20.2	8.3	22.4	1.3	3.9	149.9	6.0	*ND

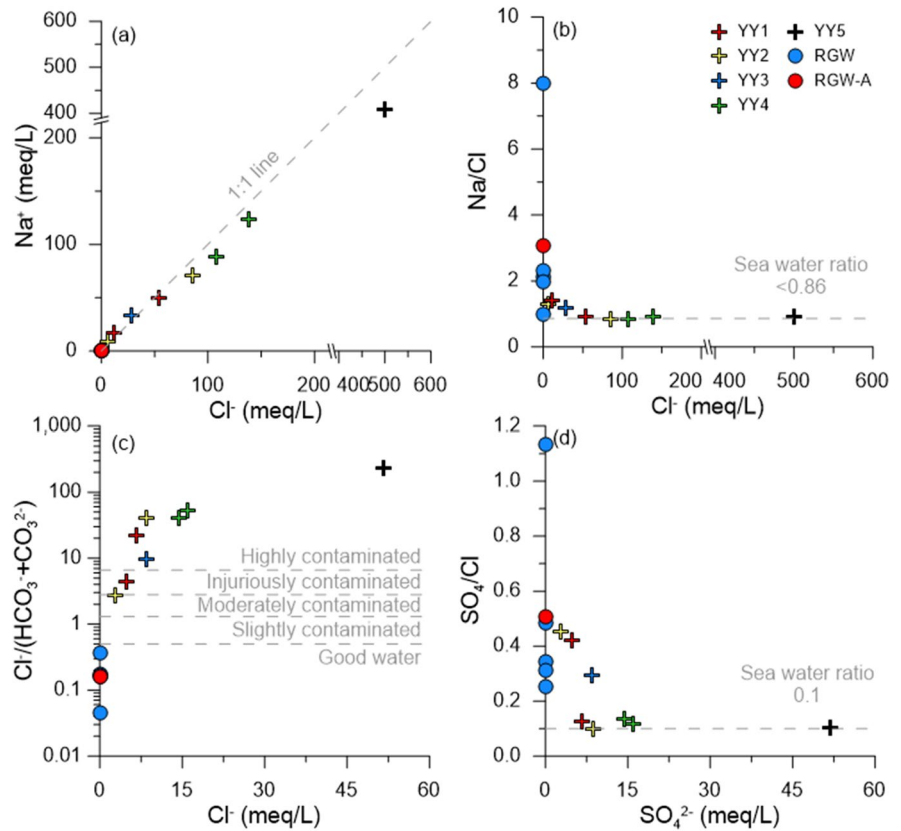
*ND not detected

by unconsolidated sedimentary layers. Additionally, there has been leakage due to the weakening of waterproofing ability during wall collapse. In the 1st field campaign, YY2 was found to be mixed with saltwater. However, in the 2nd field campaign,

YY2-2 exhibited increasing concentration of Na⁺ and Cl⁻ increased.

The ionic ratios indicated that the dissolved ions in the construction site originated from seawater (Fig. 7a). The Na/Cl ratio of seawater (YY5) is 0.91,

Fig. 7 Ionic ratios indicate seawater intrusion in the excavation site compared to the reference samples in Yangyang. **a** The 1:1 line of Na^+ and Cl^- , **b** the relationship between Na/Cl and Cl^- (seawater Na/Cl ratio from Schoeller, 1956), **c** contaminated water qualities facies suggested by Todd (1959), **d** the relationship between SO_4/Cl and SO_4^{2-}



while the Na/Cl ratio of the other samples ranged from 0.82 to 1.4. YY1, located closest to the East Sea, changed from 0.91 to 1.4. The Na/Cl ratio of YY1-2 increased while the TDS significantly decreased. It is the effect of dilution when mixed with tap water. Furthermore, the Na/Cl ratio of RGW ranged from 1.0 to 8.0. It means that RGW originated from other Na^+ sources such as ion exchange (Fig. 7b). Additionally, the water quality of the construction site ranged from moderately contaminated to highly contaminated groundwater. YY2 and YY4 become worse except YY1 because it mixed with tap water (Fig. 7c) (Todd, 1959). The RGW samples exhibit good water quality and are suitable for drinking water.

The hydrochemical characteristics of the construction site indicate a mixture with saline water, and TDS increased over time. Although groundwater levels are recovering, the groundwater is undergoing salinization. While there is a large difference in the TDS and Na^+ and Cl^- measured in mountainous areas where seawater is unaffected, there is no significant difference in NO_3^- , which is evaluated as the state of

agricultural activity (An et al., 2023). The groundwater in the study area was not polluted by anthropogenic activities (Jang et al., 2022). However, the salinization of groundwater is caused by groundwater level drop or seawater intrusion. Despite the slight rise in groundwater levels, the groundwater continues to become more saline.

The salinity of the dissolved ions in the water samples decreased at a specific point over time. It was determined that the tap water was discharged from the collapsed water pipe after the LS directly recharged the groundwater, and the total amount of dissolved ions temporarily decreased. However, as the water pipe was later closed, it was estimated that the dissolved ions at that point were directly affected by the seawater. Although it is constantly affected by seawater, it is believed that a significant amount of tap water has been recharged into sandy aquifers, temporarily deionizing the brine groundwater.

According to Banerjee & Skidar (2020), the chemistry of groundwater changes rapidly through LS. In particular, in the case of LS that occurred near the

coast and landfill points, soil and groundwater could move rapidly along with the rapid groundwater level changes. The LS generated in India appeared as a sudden or gradual LS on the surrounding surface owing to metro tunnel construction in downtown areas, causing groundwater contamination. In particular, the artificial Cl/Br ratio was found to be 288, which identified the groundwater quality caused by anthropogenic pollutants. However, in the case of Yangyang, there was no pollution source surrounding the study area except the East Sea, and the Cl⁻ concentration significantly increased in the principal component analysis, which was estimated to have led to the

inflow of seawater approximately 150 m away from the point where LS occurred.

Saltwater mixing

In coastal aquifers, fresh groundwater and saltwater mixing occurs, and the interface of the mixing zone is determined by the difference in density between saltwater and freshwater. Generally, freshwater is defined as having an EC of <2000 μS/cm, whereas seawater and brine water can be used as representative samples of saltwater. Defining the saltwater-freshwater interface is critical for sustainable long-term groundwater use.

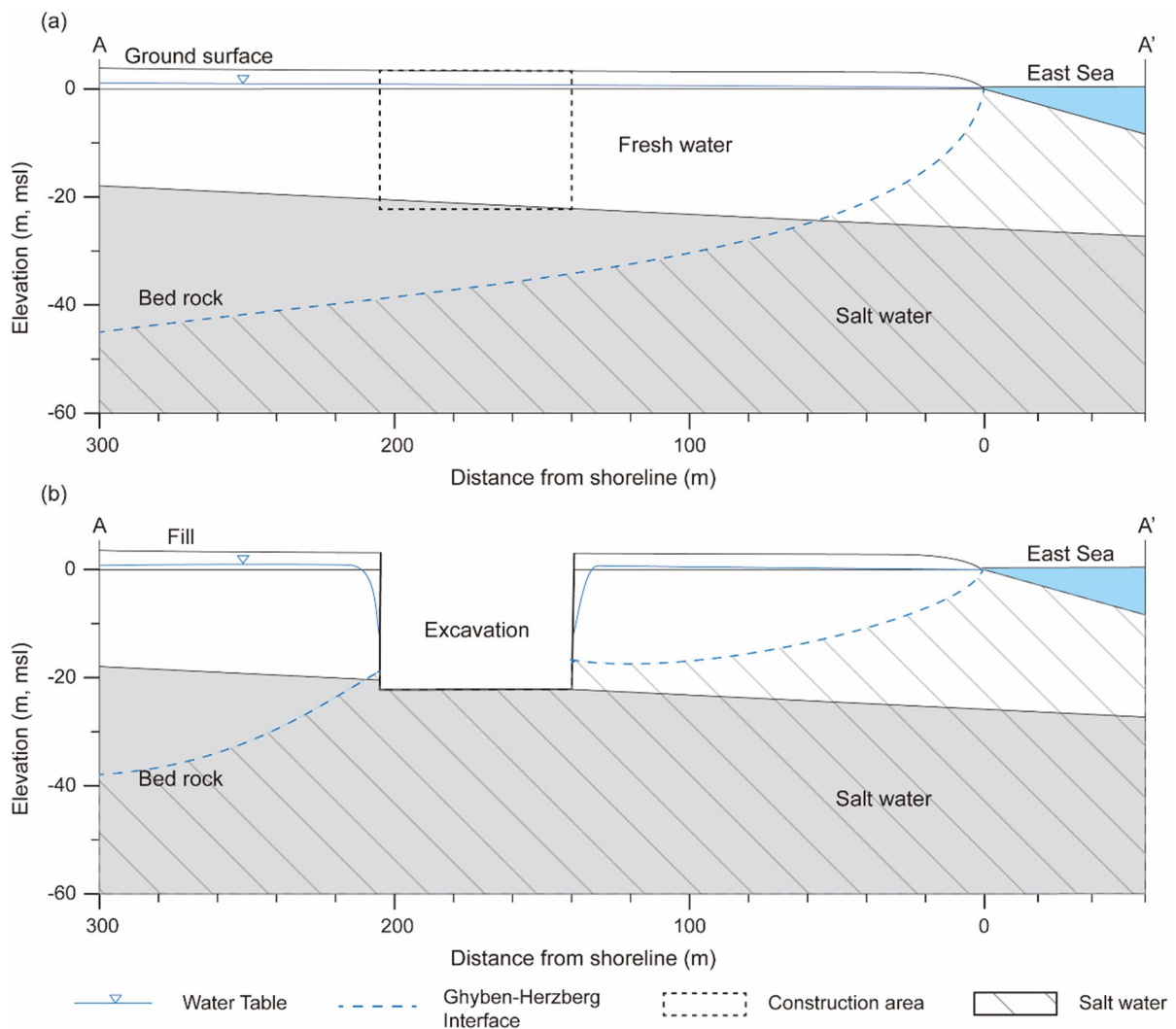


Fig. 8 Changes in groundwater level and freshwater and saltwater interface. **a** Before excavation and **b** after land subsidence

Table 3 Evolution process of groundwater and reference samples using BEX

Sample	BEX	Water process
YY1	4.40	Freshening
YY2	2.75	Freshening
YY3	8.35	Freshening
YY4	-6.62	Salinization
YY1-2	5.63	Freshening
YY2-2	-3.78	Salinization
YY4-2	3.05	Freshening
RGW1	0.81	Freshening
RGW2	0.46	Freshening
RGW3	0.54	Freshening
RGW4	0.48	Freshening
RGW5	1.48	Freshening
RGW-A	0.75	Freshening

The interface was estimated using the EC and groundwater level data (Fig. 8). The Ghyben-Herzberg interface has a normal distribution along the coast. Prior to construction, the groundwater level was between -2.51 and -2.38 m GL (0.87 to 0.99 m EL.). However, after the LS occurrence, the groundwater level in the area averaged -19.22 m GL and cannot be defined using the general Ghyben-Herzberg interface depth: The EC of W-10, the observation closest to the LS point, was >80,000 μS/cm. However, the EC measured in the sump (YY4) ranged from 13,731 to 15,487 μS/cm, which was lower than that at the LS point; however, the saltwater was steadily increasing.

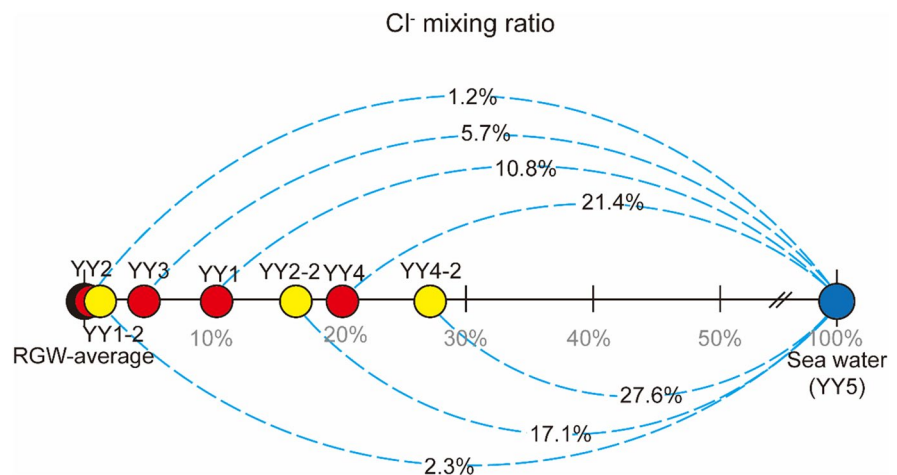
As the freshwater-saltwater interface rises above the bottom surface of the excavation area, the sump

is characterized by a significantly high EC. Consequently, the groundwater level in the area decreases vertically as it approaches the construction site, causing an increase in saltwater. However, it is assumed that the increase in EC, despite the slight rise in the groundwater level, is due to the different influence times of saltwater and groundwater (Andersen et al., 1988; Liu et al., 2017; Setiawan et al., 2023).

The RGW samples exhibited BEX values greater than 0, indicating a freshening process in the groundwater of the mountainous region (Table 3). Despite the mountainous region being distant from the East Sea, where seawater intrusion does not directly impact groundwater quality, the study area is located near the East Sea and has experienced pre-existing or frequent seawater intrusion. This intrusion has led to the salinization of coastal aquifers. However, samples YY1, YY2, and YY3 show evidence of freshening. It can be inferred that the water evolution process in this area is characterized by freshening resulting from past saltwater intrusions.

Although the increase in saltwater in the study area was estimated (Fig. 8), it was compared with seawater and the average of the reference samples used as endmembers in the Yangyang area (Fig. 9). YY4, which was assumed to be brackish at this point, was approximately 21.4 to 27.6% mixed with the East Sea and was continuously increasing. In addition, the Cl⁻ mixing ratio of YY1 discharged from the LS decreased from 10.8 to 2.3%, which was attributed to the effect of mixing of tap water due to damage to the LS. Alternatively, in the case of YY2, it increased from 1.2 to 17.1% due to the increase in brine. In the case of YY4, the change in the Cl⁻ ratio was

Fig. 9 Mixing of groundwater with seawater in the excavation site (end members are YY5 (East Sea) and average of reference samples (RGW average). And red circles mean water samples sampled on August 5, 2022, and yellow circles mean water samples sampled on August 9, 2022)



insignificant compared to the other points; therefore, it was assumed that the point was deep groundwater.

As the freshwater-saltwater interface rises above the bottom surface of the excavation area, the sump is characterized by a significantly high EC. Consequently, the groundwater level in the area decreases vertically as it approaches the construction site, causing an increase in saltwater. However, it is assumed that the increase in EC, despite the slight rise in the groundwater level, is due to the different influence times of saltwater and groundwater (Andersen et al., 1988; Liu et al., 2017; Setiawan et al., 2023).

In coastal areas, Cl^- is a good indicator for seawater intrusion, recharge, and mixing. The study area is near the East Sea and is located in a freshwater-seawater transition zone. However, it is difficult to assess groundwater flow because groundwater well and level data are depleted. Jeon et al. (2015) calculated the mixing ratio of groundwater and stream water through the exchange of water isotopes and explained the interaction between streams and groundwater in the hyporheic zone. Generally, seawater intrusion assessment uses the Cl/Br ratio; however, in this case, the reference samples were not analyzed for Br. An increase in the Cl^- mixing ratio indicates the degree of salinity contributing to the aquifer by providing values for direct saline and fresh groundwater. For seawater intrusion assessment, Cl^- can present the quantitative mixing ratio.

Conclusions

Until now, significant research has been conducted on groundwater level changes associated with LS, which has contributed greatly to clarifying its cause. In this study, the hydrogeological characteristics of the site were evaluated using groundwater level and groundwater quality data from the area where LS occurred. LS occurred on August 3, 2022, and although the groundwater level was periodically measured, there were reliability issues with the data when a new observation well was installed. However, the hydrogeological characteristics could still be evaluated using the groundwater level and water quality data measured. After approximately 1 month, the average groundwater level rose, and it was determined that the groundwater level recovered as the groundwater outflow was reinforced after the LS occurred. The water

quality at most monitoring wells deteriorated despite the rising water levels. The water quality was characteristic of coastal aquifers. During the study, the increase in TDS despite the rise in the groundwater level was considered a result of the increase in salinity at depths due to the decrease in groundwater level, rather than fast recovery by groundwater level rise. In the previous survey, Cl^- in the area near YY1 was collected. The Cl^- concentration before construction at the location where LS occurred was 292 mg/L. But in 1st field campaign, there was a significant rise in the Cl^- concentration, indicating a saltwater intrusion by the LS. It is estimated that saltwater intrusion or rising contributed to this as the groundwater level fell. In particular, the EC was the highest in YY1 when the LS occurred. This suggests that LS had a direct impact on the groundwater quality. However, it is estimated that the DO of all water samples in the excavation site is higher than East Sea (YY5), so it is not directly seawater intrusion. It is presumed that this increase was influenced by deep groundwater rather than mixing with seawater.

Excessive groundwater extraction and utilization are known to be the primary causes of LS. The LS has significant impacts on the underground environment, such as the rise of saltwater. However, the influence of LS on seawater intrusion is negligible in this study. Unfortunately, the reliability of the recorded groundwater levels in the previous study was insufficient. This limitation hindered the accurate assessment of the direct correlation between declining groundwater level and the LS. However, through continuous monitoring of the underground environment, it becomes possible to obtain a comprehensive understanding of the recovery process of the local environment. Therefore, environmental monitoring is an essential element for sustainable development and must be continued even after a geological disaster. This enables us to minimize the impact of geological disasters and continuously restore the underground environment of the region.

Author contribution JJ: investigation, methodology, data curation, conceptualization, visualization, writing—original draft, writing—review and editing. J-YL: supervision, writing—review, editing, validation, funding acquisition, and project administration. MoR: writing—review and editing. MaR: writing—review. ML: investigation, writing—review, visualization, and editing. SO: data curation, visualization, conceptualization, and writing—review and editing.

Funding This research was supported by the Basic Science Research Program through the National Research Foundation of Korea (NRF) funded by the Ministry of Education (No.2019R1A6A1A03033167).

Data availability All data generated or analyzed during this study are included in this published article.

Declarations

Ethics approval All authors have read, understood, and complied as applicable with the statement on “Ethical responsibilities of Authors” as found in the Instructions for Authors.

Consent to participate Not applicable.

Consent for publication Not applicable.

Competing interests The authors declare no competing interests.

References

- An, H., Ha, K., Lee, E., & Ko, K.-S. (2023). Analysis of groundwater quality variation characteristics using hydrogeochemical characteristics, ANOVA and trend analysis in rural areas. *Journal of the Geological Society of Korea*, 59(1), 69–89.
- Andersen, P. F., Mercer, J. W., & White, H. O. (1988). Numerical modeling of salt-water intrusion at Hallandale. *Florida Groundwater*, 26(5), 619–630.
- Bagheri-Gavkosh, M., Hosseini, S. M., Ataie-Ashtiani, B., Sohani, Y., Ebrahimian, H., Morovat, F., & Ashrafi, S. (2021). Land subsidence: A global challenge. *Science of the Total Environment*, 778, 146193.
- Banerjee, S., & Skidar, P. K. (2020). Land subsidence due to leakage of aquitard-aquifer pore water in an under-construction tunnel of East-West Metro Railway Project, Kolkata. *Journal of the Geological Society of India*, 96, 467–474.
- Cardona, A., Carrillo-Rivera, J. J., Huizar-Álvarez, R., & Graniel-Castro, E. (2004). Salinization in coastal aquifers of arid zones: An example from Santo Domingo, Baja California Sur, Mexico. *Environmental Geology*, 45, 350–366.
- CITYN (2020). Geotechnical investigation report: Underground safety impact assessment of living accommodation facility in Yangyang. CITYN, Sokcho, Korea, pp. 37–57. (in Korean).
- Galloway, D. L., & Burbey, T. J. (2011). Review: Regional land subsidence accompanying groundwater extraction. *Hydrogeology Journal*, 19, 1459–1486.
- Galloway, D. L., Jones, D. R., & Ingebritsen, S. E. (1999). Land subsidence in the United States. *U.S. Geological Survey Circular*, 1182, 7–13.
- Galloway, D. L., Erkens, G., Kuniatsky, E. L., & Rowland, J. C. (2016). Preface: Land subsidence processes. *Hydrogeology Journal*, 24, 547–550.
- Gong, S. L., Li, C., & Yang, S. L. (2009). The microscopic characteristics of Shanghai soft clay and its effect on soil body deformation and land subsidence. *Environmental Geology*, 56(6), 1051–1056.
- Guzy, A., & Malinowska, A. A. (2020). State of the art and recent advancements in the modelling of land subsidence induced by groundwater withdrawal. *Water*, 12, 2051.
- Herrera-García, G., Ezquerro, P., Tomás, R., Béjar-Pizarro, M., López-Vinielles, J., Rossi, M., Mateos, R. M., Carreón-Freyre, D., Lambert, J., Teatini, P., Cabral-Cano, E., Erkens, G., Galloway, D., Hung, W. C., Kakar, K., Sneed, M., Tosi, L., Wang, H., & Ye, S. (2021). Mapping the global threat of land subsidence. *Science*, 371(6524), 34–36.
- Jang, J., Lee, J.-Y., Oh, S., & Kim, Y.-I. (2022). Evaluation of hydrochemical characteristics and hydraulic connectivity using fluorescent mineral tracer test in karst region of Samcheok. *Korea, Journal of the Geological Society of Korea*, 58(3), 347–360.
- Jeen, S.-W., Kang, J., Jung, H., & Lee, J. (2021). Review of seawater intrusion in western regions of South Korea. *Water*, 13(6), 761.
- Jeon, W.-H., Lee, J.-Y., Cheong, W.-Y., Park, Y.-H., Oh, S.-H., Eum, D.-H., & Park, J.-Y. (2015). A multi-method approach revealing the groundwater-stream water interaction in the Inbuk stream, Korea. *Geoscience Journal*, 19, 325–340.
- Jiao, J., & Post, V. (2019). *Coastal hydrogeology*. Cambridge University Press.
- Liu, B., Liao, Y., Yan, S., & Yan, H. (2017). Dynamic characteristics of saltwater intrusion in the Pearl River Estuary, China. *Natural Hazards*, 89, 1097–1117.
- Marfai, M. A., & King, L. (2007). Monitoring land subsidence in Semarang, Indonesia. *Environmental Geology*, 53, 651–659.
- Michael, H. A., Post, V. E. A., Wilson, A. M., & Werner, A. D. (2017). Science, society and the coastal groundwater squeeze. *Water Resources Research*, 53, 2610–2617.
- MoE & K-water (2021). Basic Survey Report of Groundwater in Yangyang, *Ministry of Environment and K-water*, Sejong, Korea, pp. 135–175. (in Korean).
- Orhan, O. (2021). Monitoring of land subsidence due to excessive groundwater extraction using small baseline subset technique in Konya. *Turkey. Environmental Monitoring and Assessment*, 193, 174.
- Park, C.-H., Huh, S., Jou, H.-T., Hong, J.-K., & Isezaki, N. (1997). Geological interpretation based on magnetic anomalies and seismic data offshore Yangyang-Samchuk, the East Sea of Korea. *Journal of the Geological Society of Korea*, 33(3), 117–126.
- Phien-vej, N., Giao, P. H., & Nutalaya, P. (2006). Land subsidence in Bangkok, Thailand. *Engineering Geology*, 82(4), 187–201.
- Piper, A. M. (1944). A graphical procedure in the geochemical interpretation of water-analysis. *EOS, Transactions American Geophysical Union*, 25(6), 914–928.
- Raza, M., & Lee, J.-Y. (2019). Factors affecting spatial pattern of groundwater hydrochemical variables and nitrate in agricultural region of Korea. *Episodes*, 42(2), 135–148.
- Schoeller, H. (1956). Geochimie des eaux souterraines application aux eaux de gisements de pétrole. *Revue De L'institut Français Du Pétrole Et Annales Des Combustibles Liquides*, 10, 219–246.

- Setiawan, I., Morgan, L. K., & Doscher, C. (2023). Saltwater intrusion from an estuarine river: A field investigation. *Journal of Hydrology*, *617*, 128955.
- Shen, J., Wu, Q., & Liu, W. (2020). The development of the water-richness evaluation model for the unconsolidated aquifers based on the extension matter-element theory. *Geotechnical and Geological Engineering*, *38*, 2639–2652.
- Shi, X., Jiang, S., Xu, H., Jiang, F., He, Z., & Wu, J. (2016). The effects of artificial recharge of groundwater on controlling land subsidence and its influence on groundwater quality and aquifer energy storage in Shanghai. *China Environmental Earth Science*, *75*, 195.
- Shirzaei, M., Freymueller, J., Törnqvist, T. E., Galloway, D. L., Dura, T., & Minderhoud, P. S. (2021). Measuring, modelling and projecting coastal land subsidence. *Nature Reviews Earth & Environment*, *2*(1), 40–58.
- Song, K. -Y., Park, S. -I. & Jo, D. -L., (2011), Geological report of the Sokcho-Yangyang sheet (scale 1:50,000). *Korea Institute of Geoscience and Mineral Resources (KIGAM)*, Daejeon, Korea, pp. 6–52. (in Korean with English summary).
- Stuyfzand, P.J. (2008). Base-exchange indices as indicators of salinization or freshening of (coastal) aquifers. In Proceedings of 20th Salt Water Intrusion Meeting. Florida, June 23–27. pp. 262–265.
- Terzaghi, K. (1925). Principles of soil mechanics, IV—Settlement and consolidation of clay. *Engineering News-Record*, *95*(3) 874–878.
- Todd, D. K. (1959). *Groundwater Hydrology* (1st ed.). Wiley.
- Wei, Z. X., Zhai, G. Y., & Yan, X. X. (2010). *Atlas of Shanghai urban geology*. Geology Press.
- Wu, Y.-X., Lyu, H.-M., Shen, J.S., & Arulrajah, A. (2018). Geological and hydrogeological environment in Tianjin with potential geohazards and groundwater control during excavation. *Environmental Earth Sciences*, *77*, 392.
- Xu, Y. S., Shen, S. L., Cai, Z.-Y., & Zhou, G.-Y. (2008). The state of land subsidence and prediction approaches due to groundwater withdrawal in China. *Natural Hazards*, *45*, 123–135.
- Xu, Y.-S., Ma, L., Du, Y.-J., & Shen, S.-L. (2012). Analysis of urbanisation-induced land subsidence in Shanghai. *Natural Hazards*, *63*, 1255–1267.
- Xu, Y.-S., Shen, S.-L., Ma, L., Sun, W.-J., & Yin, Z.-Y. (2014). Evaluation of the blocking effect of retaining walls on groundwater seepage in aquifers with different insertion depths. *Engineering Geology*, *183*, 254–264.
- Xu, Y.-S., Wu, H.-N., Wang, B.Z.-F., & Yang, T.-L. (2017). Dewatering induced subsidence during excavation in a Shanghai soft deposit. *Environmental Earth Science*, *76*, 351.
- Yan, X., Xu, Y., Yang, T., Tosi, L., Stouthamer, E., Minderhoud, P., Teatini, P., Kooi, H., Andreas, H., Pradipta, D., Donnici, S., & Boni, R. (2022). Sustainable development of coastal cities through control of land subsidence: Activities of IGCP Project 663 in Jakarta. *Episodes*, *45*(1), 101–108.

Publisher's note Springer Nature remains neutral with regard to jurisdictional claims in published maps and institutional affiliations.

Springer Nature or its licensor (e.g. a society or other partner) holds exclusive rights to this article under a publishing agreement with the author(s) or other rightsholder(s); author self-archiving of the accepted manuscript version of this article is solely governed by the terms of such publishing agreement and applicable law.